KEK Belle Note #135
August 26, 1996

Flow Control and Measurement for RPC Gases

Belle Note # 135

M. Ahart, R. Fertig, K. Korotushenko, and D. Marlow
Princeton University

1 Introduction

The BELLE RPC system will comprise of order 1000 independent gas volumes. We know from experience that it is best avoid connecting too many volumes in series, since the gas quality appears to deteriorate as it flows through an operating RPC. Although independently supplying a large number of volumes is not a fundamental problem, it does present at least two practical challenges: i) a simple way to evenly apportion gas between the channels is needed, and ii) a way to automatically monitor the flow rate to each channel is required.

The first requirement could be met by instrumenting each channel with an adjustable valve, but owing to the rather low flow rate per channel, high quality (and therefore costly) valves would be required. Moreover, adjusting each valve would be a tedious process, made even more difficult by the fact that the total gas flow is fixed by the setting of the mass flow controllers used for gas mixing.

As an alternative to adjustable valves, we propose placing fixed-impedance "flow resistors" formed from stainless-steel tubes with very small inner diameters upstream of each RPC. To the extent that the pressure drops across these tubes are the same and large compared to the typical chamber output pressure (i.e., a few mm of oil above atmosphere), the gas flow to each RPC should be the same.

Traditionally, the second requirement has been met by using output bubblers, which provide a simple qualitative measure of the flow rate, and also serve to maintain the chambers at a slight positive pressure with respect to the ambient atmosphere. Such bubblers can be readily fabricated at low cost or purchased commercially for about \$ 20 each. However, it is unrealistic to expect that more than a few dozen bubblers can be visually monitored in a systematic way over the lifetime of BELLE. A system with an electronic readout is obviously superior in this regard. We therefore propose to construct bubblers instrumented with a simple photogate device that generates a pulse with the passage of each bubble. This approach will not only confirm that the gas flow to each RPC is stable, but will also afford a semiquantitive measure of the gas flow rate, that will help to verify that there are no gas leaks—an important safety consideration.

In this note, we describe proof-of-principle laboratory measurements on prototype devices.

2 Minimum and Maximum Flow Requirements

The volume of a typical barrel RPC is $220 \times 220 \times 0.2$ cm$^3 \approx 10^4$ cc. The largest flow rates will occur during startup, when it would be desirable to flow enough gas for one volume change per hour, or about 170 cc/min. In steady state operation, one volume change every two days would be more appropriate. This corresponds to a flow rate of 3.5 cc/min.

3 Flow Resistors

The flow resistors consist of 10-cm-long 1.5 mm-diameter stainless steel tubes that have inner diameters ranging from 127 to 508 μm. They can be purchased from scientific supply companies for about two dollars each. For these tests, we attached polyflow gas fittings to each end using 5-minute epoxy.

3.1 Flow Rate Theory

When a viscous fluid undergoes laminar flow through a tube, a pressure gradient proportional to the volume flow rate is set up between the ends of the tube according to Poiseuille's law,

$$\frac{dV}{dt} = \frac{\pi}{8} \frac{R^4}{\eta} \frac{\Delta p}{L} \tag{1}$$

where R is the radius of the tube, L is the length of the tube, η is the coefficient of viscosity of the fluid, and Δp is the difference in pressure between the ends of the tube. By measuring the ratio of the pressure difference to the flow rate for various values of R, we can determine the value of R necessary to produce the desired ratio.

3.2 Flow Rate Measurements

Using the MKS instruments multi gas controller's mass flow controller, argon gas was pumped into the flow resistor at constant rates. A pressure meter was connected to the flow controller side of the flow resistor, while the other side exhausted to the lab room, at atmospheric pressure. Using flow resistors of inner diameter .007 in = 178 μm, .01 in = 254 μm, and .02 in = 508 μm, the pressure difference was recorded for various values of the flow rate. A typical pressure *vs.* flow curve is shown in figure 1. As predicted, the relationship is linear.

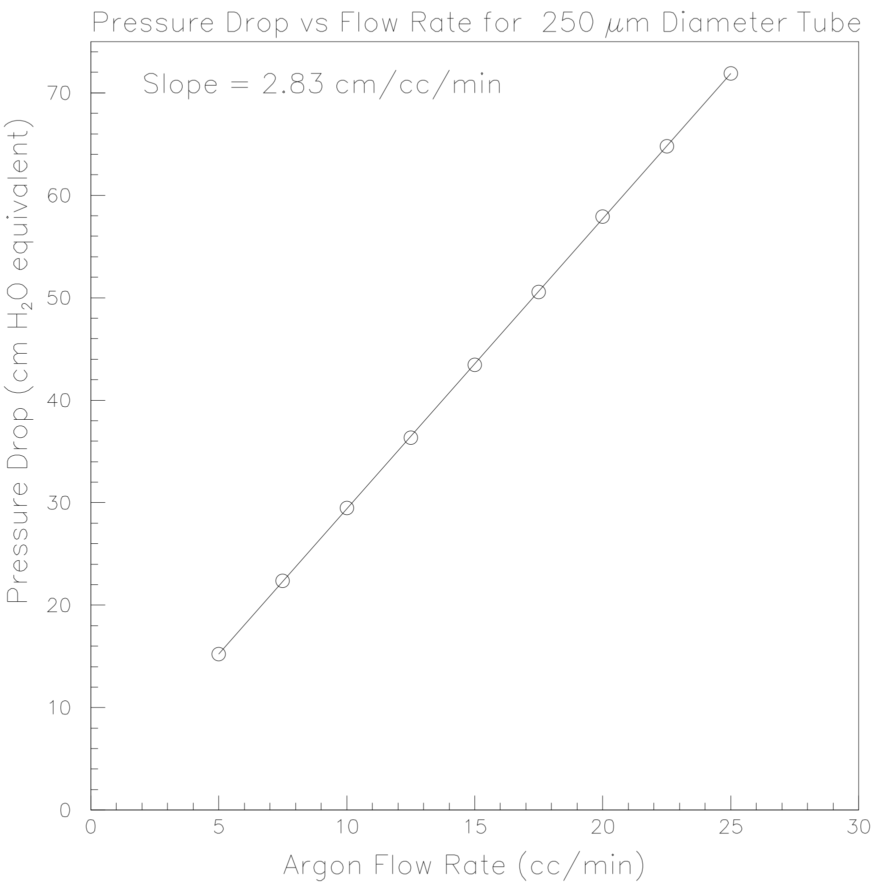

Figure 1: Pressure drop *vs.* flow rate for a 250 μm diameter flow resistor.

Similar measurements were made for flow resistors of other diameters. Using their experimentally determined slopes, a graph of the ratio vs. $1/R^4$ was plotted. The data were found to agree well with the $1/R^4$ scaling predicted by Poiseuille's law (see figure 2). Rearranging Poiseuille's law, we have

$$\eta = \frac{\pi}{8} \frac{m}{L} \tag{2}$$

where m is the slope in figure 2. The coefficient of viscosity obtained using $L = 10$ cm is 172 μpoise, which is within 25% of the actual value for argon, 221 μpoise.

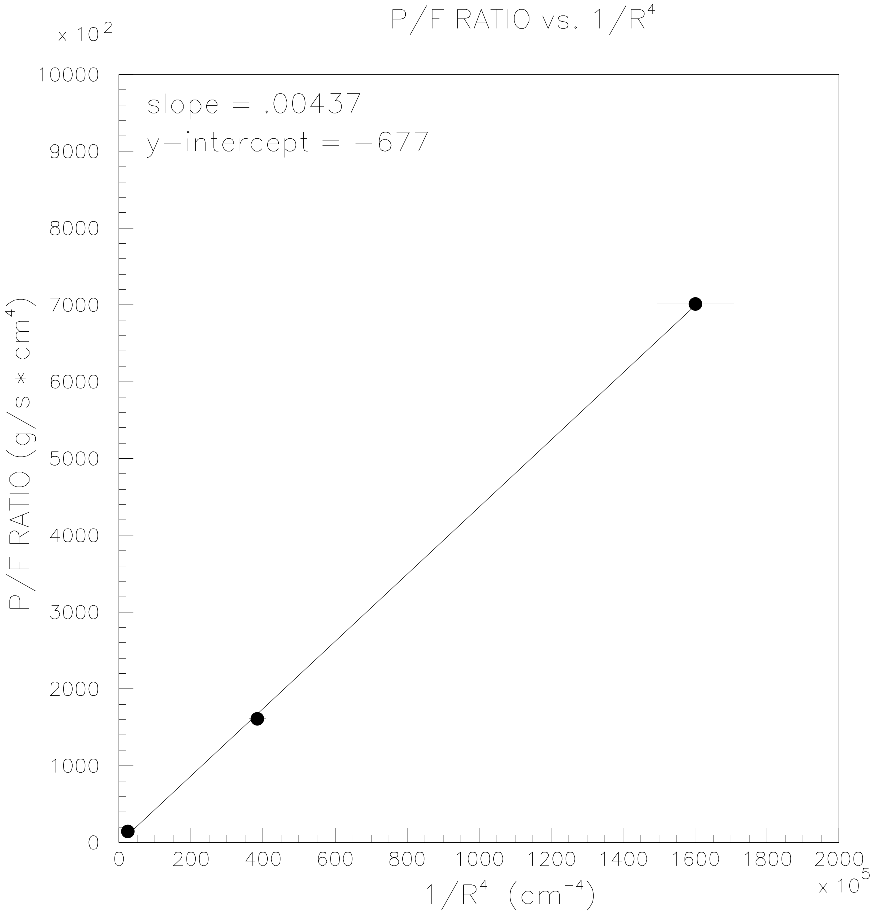

Figure 2: Pressure/flow ratio *vs.* $1/R^4$.

This discrepancy may have been due to very small gas leakage or mixing of air with the argon gas. To test for leakage the exhaust valve and entrance valve were both shut off after gas had accumulated in the tubing. After five minutes observation there was no apparent leakage. Since the smallest observable pressure change on the meter was 0.1 inches of water, the maximum possible pressure leakage rate was approximately .02 inches water/min. In comparison, when the entrance valve was shut but the exit valve left open, the preasure leakage rate was close to 1 inch of water/s. Using

$$\frac{\Delta F}{F} = \frac{dP/dt_1}{dP/dt_2} \qquad (3)$$

we find a maximum of 2% error, which would not create a 25% error in η.

In order to determine whether the second effect was present, the system was left on overnight, allowing all air to exhaust. There was no change. Thus neither leaks nor air contamination can explain the discrepancy.

A third possibility is that the inner radii of the tubes differs from their nominal values. Since the inferred viscosity goes as the fourth power of the assumed radius, a relatively small error could account for difference. Although did we not attempt a direct measurement of the inner diameters of the tubes, we were able to estimate the unit-to-unit variations by measuring the pressure-to-flow ratio for several tubes. In particular, five 175-μm and five 250-μm tubes were measured. For each tube pressure drop measurements were made for five different flows. The tabulated values are the pressure drop for a flow of 1 cc/min. Thus for Sample #1 of the 175 μm-diameter flow resistor a prssure head of 12.7 cm of water equivalent would be required to sustain 1 cc/min of flow. By way of comparison we note that the same pressure difference across an RPC would produce a flow of roughly 150 cc/min (i.e., the flow impedance of the RPC is 150 times smaller). The resulting slopes are summarized in table 1. The tube-to-tube variations are at the 15% to 20% level and may well explain the discrepancy. In any event, the general agreement between theory and experiment is quite adequate for our purposes.

4 Digital Bubbler

4.1 Design & Operation

The digital bubbler system consists of two components, one mechanical and one electrical. The mechanical component (see figure 3) is a clear plastic cube approximately 2.5 cm on each side with an oil (or water) filled cavity in the center. A small hole in the bottom of the cavity leads under the cube to a gas input connector. An opto-transistor photogate (QT Type H22A1), whose leads are routed to the outside of the cube is immersed in the oil. The photogate consists of an light emitting diode (LED) and a phototransistor, separated by a 3.1 mm gap. It is situated directly above the hole at the bottom of the cavity so that bubbles pass through the gap separating the LED and the phototransistor, momentarily interupting the light beam.

Table 1: Measured values of $dP/(dV/dt)$ (pressure drop divided by flow rate. Pressure is measured in units of cm of water equivalent and flow is in cc per minute.

	Diameter	
Sample	175 μm	250 μm
1	12.7	2.51
2	13.1	2.90
3	12.3	3.71
4	12.1	3.00
5	18.7	3.72
$\mu \pm \sigma$	13.8 ± 2.5	3.17 ± 0.48

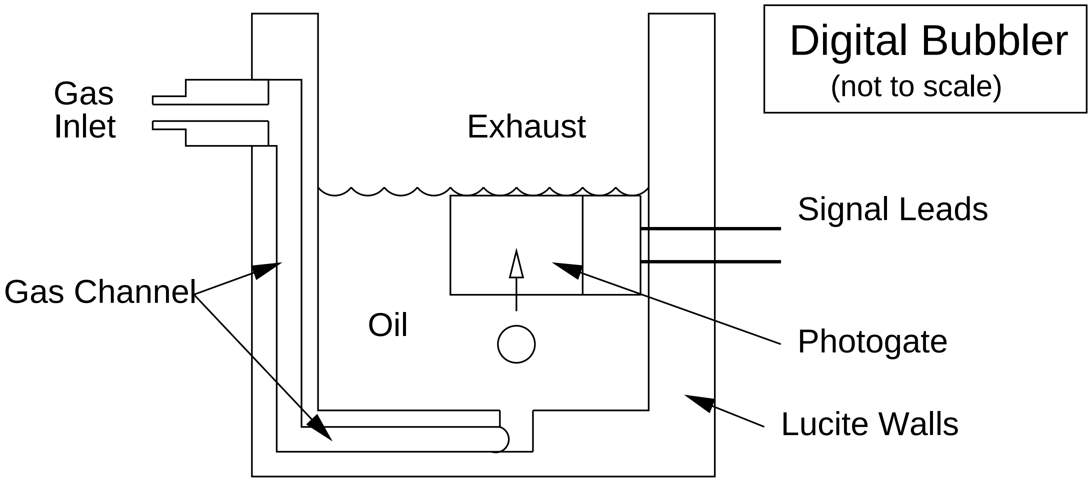

Figure 3: Sketch of prototype bubbler. The drawing is not to scale.

The circuit of the photogate and a simplified version of its readout are shown in figure 4. Light from the LED causes base current to flow in the phototransistor, which in turn causes a collector current to flow. This current causes a voltage drop across R_C. The value of R_C is chosen such that the phototransistor is in, or is close to, saturation (i.e., $V_C < 1$ V). If an object comes between the LED and the phototransistor, the photocurrent drops, causing its collector voltage to rise above the comparator threshold.

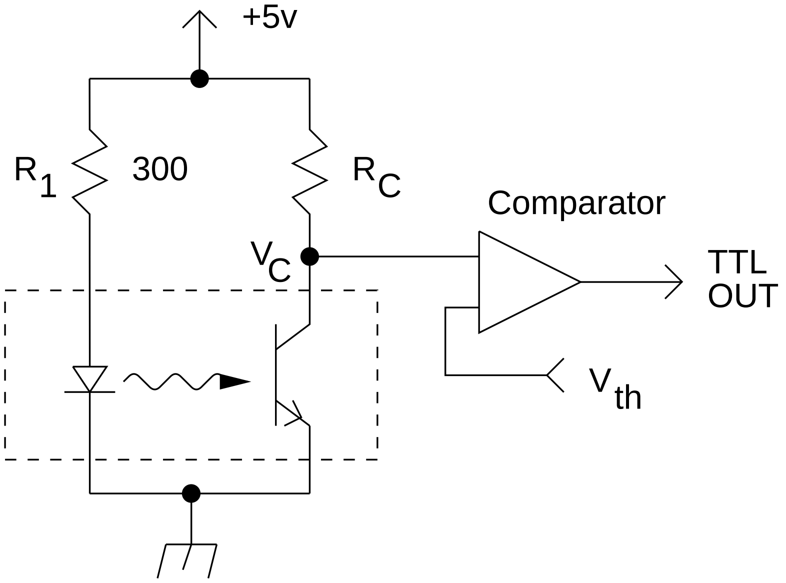

Figure 4: Simple version of the sensor readout.

4.2 Results

Figure 5 shows the response of the system to a single bubble. Note that the bubble actually causes less photocurrent to flow (in figure 5, higher voltage means less light). In any event, the signal is large and free from noise. Evidently the main effect of its passage is refraction at the oil-gas interface (hence the double-lobed pulse shape). Assuming that this is the case, we can immediately infer a bubble transit time of 200 ms. Similar observations with a water filled bubbler yielded a bubble transit time of 50 ms, presumably a result of water's lower viscosity.

Using a somewhat modified version of the circuit shown in figure 4 (see Section 4.3 below), the bubble frequency was measured for a number of different flow rates. The results are plotted in figure 6. The correlation between flow and bubble rate is clear, although there is a distinct nonlinearity. The reason for this is not yet understood,

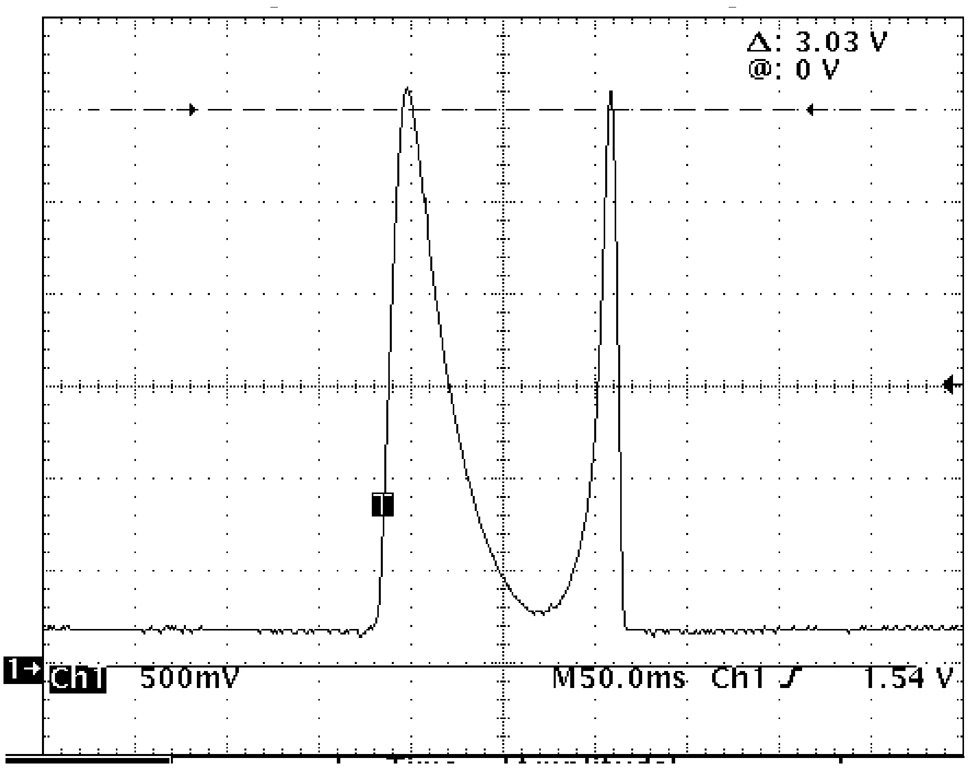

Figure 5: Scope trace showing voltage at phototransistor collector as bubble passes through the photogate. The gas was argon and the bubbler was filled with oil.

however, from visual observation of the bubbles it seems likely that there are non-neglibible "wake effects" that begin to play a role when the bubble width and the bubble spacing are of the same order.

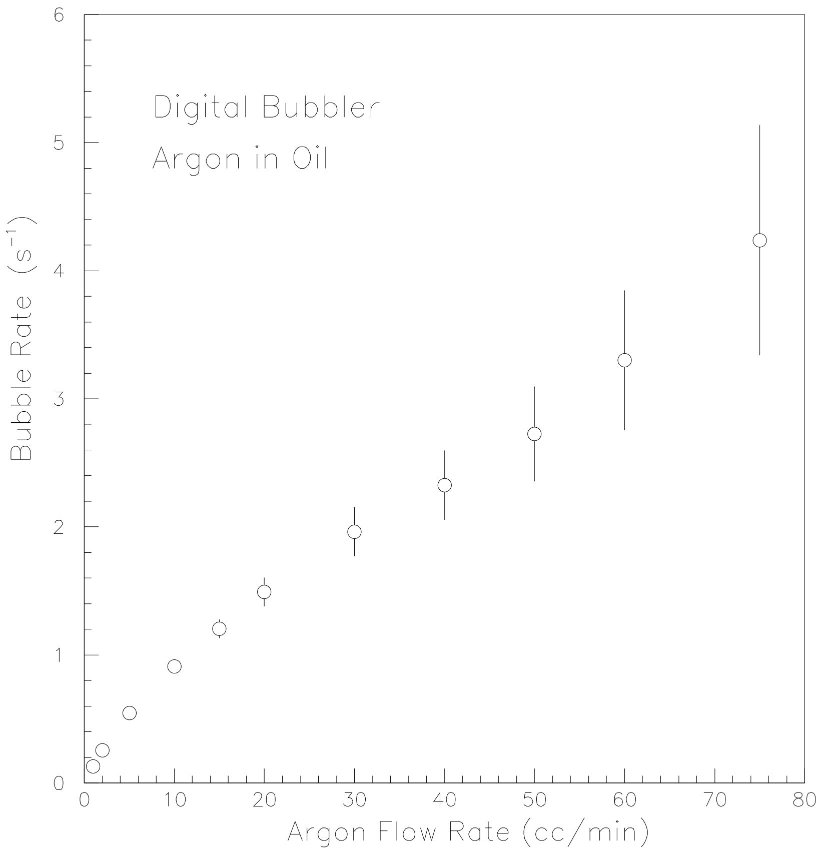

Figure 6: Bubble frequency *vs.* flow rate for argon in an oil-filled bubbler.

4.3 Circuit Refinement

A potential problem with the circuit of figure 4 is that component variations may lead to large variations in the quiescent value of V_C. Although it is a simple matter to adjust either R_1 or R_C to compensate, the need to do so would be a nuisance in a system with many channels.

An improved circuit is shown in figure 7. The voltage from the collector of the phototransistor is fed back around through a low pass filter to a Darlington-style emitter follower, which drives the LED. The feedback ensures that the quiescent value of V_C will be about 1.2 V (two diode drops). If for some reason the photocurrent drops causing V_C to increase, the Darlington pair will be turned on harder, causing the LED current to increase. If the photocurrent increases, the opposite occurs. The low-pass filter serves to disable the feedback for the relatively short signal pulses.

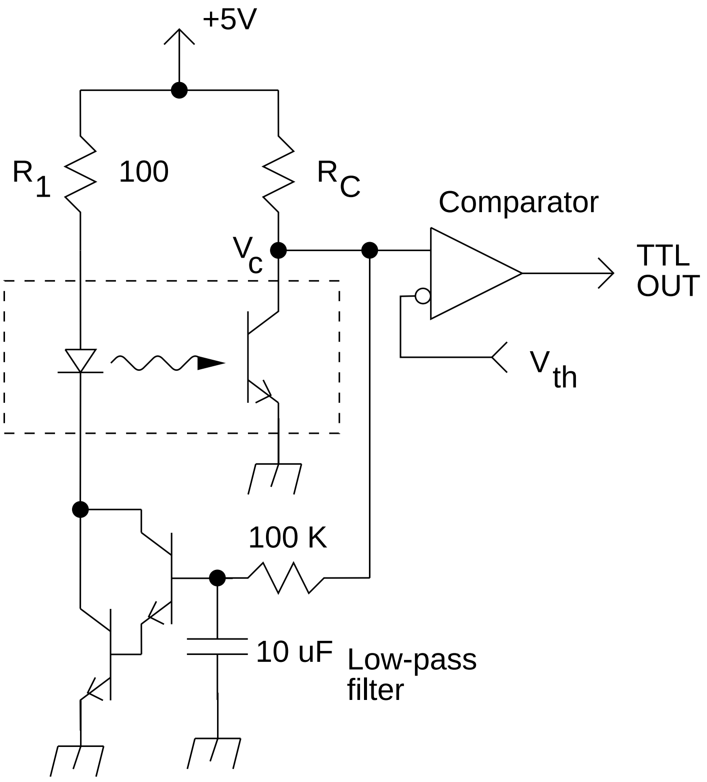

Figure 7: Sensor readout modified to include DC feedback.

To test this circuit's sensitivity to component variations, we tried several different values of R_C. Figure 8 shows the quiescent voltage and the peak pulse voltage as a function of R_C. Note that for a comparator threshold of 2 V, stable operation over a wide range of values ($0.5 < R_C < 40\ K\Omega$) is possible.

5 Discussion and Conclusions

The measurements just described indicate that both the flow resistors and the digital bubblers will work in the BELLE RPC application. There are, however, some outstanding issues that will require further study.

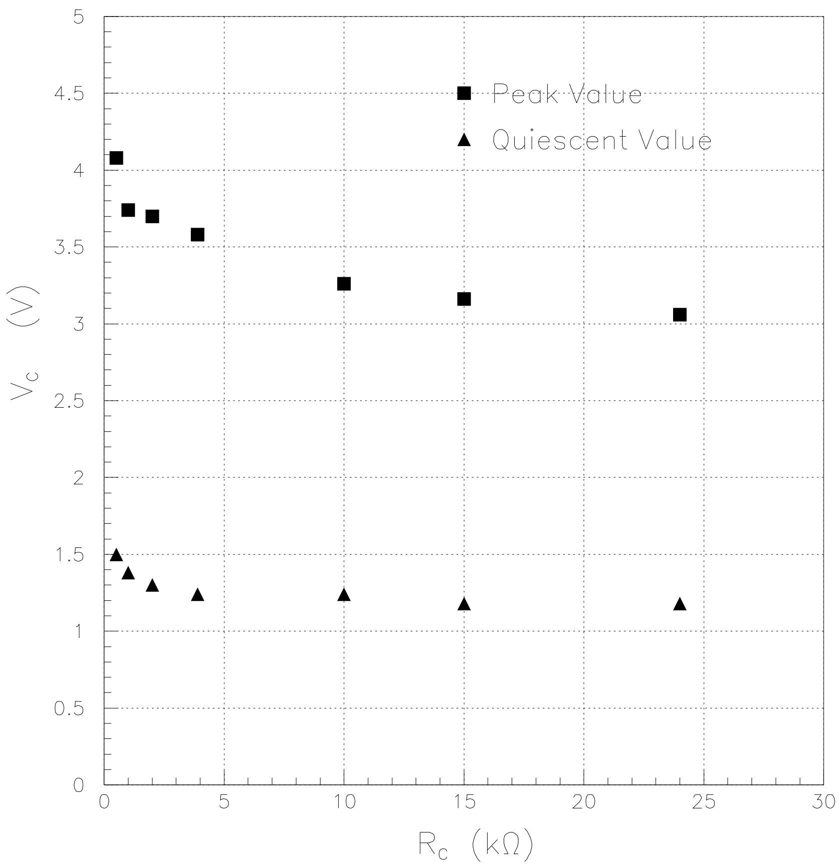

Figure 8: Quiescent and peak pulse voltages for *vs.* collector resistor value for the sensor circuit using feedback.

- The flow resistors exhibit unit-to-unit variations at the 20% level (based on the measurement of five samples of two different diameters). Although this is acceptable, a larger sample is needed to better quantify the level of the variations and to try to gain some idea of the shape of the distribution. One simple solution is to purchase more flow resistors than are needed and to remove tubes with flow resistance values far from the average.

- A more serious question is the long-term stability of the flow resistors, in particular, their susceptibility to blockage over long times. Although they can be mounted outside of the detector and fairly easily replaced, it would clearly be unpleasant to need to do this for a large number of tubes. Long term tests, which can be accelerated by using high flow rates, are in order. Presumably this problem (if it exists at all) can be mitigated by filtering of the gas, something that ought to be done in any event.

- Choice of flow resistor diameter. As noted in Section 2, the minimum flow rate is driven by the need to periodically refresh the RPC gas. Although aging tests at most labs indicate a fairly clear gas poisoning effect, precisely where this sets in is not firmly established. Although it is tempting to choose the 250 μm-diameter flow resistors since they will allow a larger *maximum* flow rate and presumably would prove less prone to clogging, their flow resistance might not be high enough to permit stable regulation of very low flows. For example, if through experience, we learn that one volume change a week (about 1 cc/min) is adequate, 175 μm tubes would be a better choice. I.e., according to table 1, the pressure drop across a typical 175 μm tube at that flow rate would be 14 cm, large compared to the oil depth of the output bubblers. On the other hand, the drop for a 250 μm tube would be only 3.2 cm, which might lead to channel-to-channel variations.

- Digital bubbler design. Although the initial digital bubbler design worked surprisingly well for a first attempt, a number of improvements are needed. In particular, a somewhat larger bubble size would be useful, since that would (presumably) increase the maximum flow rate that could be accurately measured (about 20 cc/min with the current model). (One puzzle is that from figure 6 we infer a bubble diameter of approximately 7 mm, seemingly larger than what one might guess from visual observation, and quite a bit larger than the 3-mm berth of the photogate. This may in fact suggest that a wider gate would be beneficial.)